Progress in the microscopic description of nucleon-nucleus elastic scattering at low-energy

T. V. Nhan Hao

Faculty of Physics, University of Education, Hue University, 34 Le Loi Street, Hue City, Vietnam

D. Quang Tam

Faculty of Basic Science, University of Medicine, Hue University, Hue City, Vietnam

Received (received date)
Revised (revised date)

In this brief report, we make a short review of progress in developing the microscopic optical potential in recent years. In particular, we present our current studies and future plans on building the microscopic optical potential based on the so-called nuclear structure models at low-energies.

1. Introduction

In nuclear physics studies we still have two unsolvable problems: the many-body problem and the nuclear interaction. To avoid these difficulties, the phenomenological approaches are the most efficient ways to describe the nuclear systems, for example, the great success of the using phenomenological effective interaction in nuclear structure and phenomenological optical potential in nuclear reactions. However, the limit of the phenomenological approaches is the unexpected separation between the structure and reactions communities. Also, due to the fits with experimental data, these approaches do not have the prediction powers, especially for the nuclear reactions off targets outside the range of validity of the fits, e.g., in the case of the exotic nuclei produced in r-process. Microscopic optical potential is expected to have the prediction powers but also is the link between the nuclear structure and reactions studies. This link allows us to learn the Physics meaning from the analysis of the experimental data from the nuclear reactions studies.

In the last 5 years, huge efforts have been devoted to develop the microscopic optical potential. This potential is identified with the nucleon self-energy $\Sigma(r, r', E)$ which is a complex non-local energy-dependent function. When the incident energy $E > 0$, $\Sigma(r, r', E)$ is the nuclear optical potential. For bound states with $E < 0$, the real part of $\Sigma(r, r', E)$ represents the shell model or mean-field potential. We could list the most efficient methods to calculate this self-energy: *ab initio* approaches [1,2], nuclear matter approaches [3–8], nuclear structure approaches [9–13, 15–19].

Recently, the combination the Green's function approach with the couple-cluster

method [2] has been used to generate the microscopic optical potential for neutron elastic scattering of ^{40}Ca and ^{48}Ca. This success is based on the progress of the *ab initio* nuclear reaction community in many aspects: mass number, precision and accuracy. They can now have the reliable predictions for nuclei as heavy as ^{120}Sn by using the modern nucleon-nucleon (NN) and three-nucleon forces (3NFs) from chiral effective field theory. In Ref. [2], the microscopic optical potential is defined as

$$\Sigma' \equiv \Sigma^* + U, \tag{1}$$

where $\Sigma^*(\gamma, \delta, E)$ is the self-energy which can be calculated by

$$\Sigma^*(E) = [G^{0)}(E)]^{-1} - G^{-1}(E), \tag{2}$$

where U is the HF potential, and the Green's function G fulfills the Dyson equation

$$G(\alpha, \beta, E) = G^{(0)}(\alpha, \beta, E) + \Sigma^{(0)}_{\gamma,\delta}(\alpha, \gamma, E) \times \Sigma^*(\gamma, \delta, E) G(\delta, \beta, E) \tag{3}$$

where $G^{(0)}$ is the first-order approximation to the Green's function. To get the optical potential, the Dyson equation has been obtained by inverting each elements within the coupled-cluster method. The method has been applied to describe the optical potential associated with the bound states in ^{41}Ca and ^{49}Ca and the neutron scattering. Some encouraging results have been shown in comparing with the phenomenological Koning-Delaroche potential. However, due to the complicated structure of the equation (2), the imaginary part (the absorption from the non-elastic channel) of the optical potential has been dropped.

Another way to calculate the nucleon self-energy is to use the nuclear matter approach [3, 4]. Since this method is only valid for the infinite nuclear matter, the local density approximation has been used. To get the local optical potential, the solution of the self-consistent equation has been folded with the resulting density-dependent mean-field with a realistic point-nucleus density distribution. In this approach, the first order of Σ is the Hartree-Fock contribution

$$\Sigma^{(1)}_{\rm HF}(q, \omega; k_f) = \sum_l \langle \mathbf{q h_1} s s_1 t t_1 | \tilde{V}_{2N} | \mathbf{q h_1} s s_1 t t_1 \rangle n_1 \tag{4}$$

which is real, energy-independent, and $\tilde{V}_{2N}$ is the anti-symmetrization of V_{2N}.

The second order $\Sigma^{(1)}_{\rm HF}(q, \omega; k_f)$ which is both a real and imaginary part. The direct and exchange terms are calculated from the particle states above the Fermi level

$$\Sigma_{\rm 2N}^{(2a)}(q,\omega;k_f)=\frac{1}{2}\sum_{123}\frac{|\langle \mathbf{p}_1\mathbf{p}_3 s_1 s_3 t_1 t_3|\tilde{V}_{2N}|\mathbf{q}\mathbf{h}_2 s s_2 t t_2\rangle|^2}{\omega+\epsilon_2-\epsilon_1-\epsilon_3+i\eta}\bar{n}_1 n_2 \bar{n}_3(2\pi)^3\delta(\mathbf{p}_1+\mathbf{p}_3-\mathbf{q}-\mathbf{h}_2) \tag{5}$$

where $\bar{n}_k = 1 - n_k$.

Within the above formalism, the microscopic optical potential calculations have been applied to study the real and imaginary part for incident energies lower than 100 MeV. However, no comparison with experimental data has been done. Also, as well known, the local density approximation cannot capture the physics of the collective surface modes, shell structure effects, and the spin-orbit interaction. Later, several improvements have been proposed. The improved local density approximation has been used to take into account the nonzero range of the nuclear force. The calculation of the neutron elastic scattering off ^{40}Ca have been performed at energies from 3.2 MeV up to 185 MeV. Good agreement with experimental data have been obtained except in the resonances regions. However, the absorption of the imaginary part is still too large and the spin-orbit interaction is still an intricate difficulty of the nuclear matter model based.

Another way to calculate is to use the *ab initio* calculations based on the no-core shell model using the saturating nuclear forces [1]. The Hamiltonian of the system is

$$H(A)=\hat{T}-\hat{T}_{\rm c.m.}(A+1)+\hat{V}_2+\hat{V}_3 \tag{6}$$

where $\hat{T}$ is the kinetic energy operator, and $\hat{V}_2$, $\hat{V}_3$ are the two-body and three-body interactions. The partial wave decomposition of the self-energy which is the optical potential is

$$\Sigma^{l,j}(k,k';E,\Gamma)=\sum_{n,n'}R_{n,l}(k)\Sigma^{\star,l,j}_{n,n'}(E,\Gamma)R_{n',l}(k') \tag{7}$$

which is energy-dependent, nonlocal and in a separable form, and the irreducible self-energy $\Sigma^\star(\omega)$ is the solution of the Dyson equation

$$g(\omega)=g^0(\omega)+g^0(\omega)\Sigma^\star(\omega)g(\omega) \tag{8}$$

where $g^0(\omega)$ is the free particle propagator.This model has been applied to describe the neutron elastic scattering off ^{16}O (^{40}Ca) at 3.286 (3.2) MeV respectively. The obtained results are comparable with experimental data quantitatively. However, the main drawback of this model is that the important collective states of the targets such as low-lying states and giant resonances can not be described.

Based on the same Green function method, the nuclear structure model explicitly includes the effects of collective states in which one uses two-body effective NN interactions together with some nuclear structure models to calculate the MOPs. As

the recent energy-density-functional structure approaches have proven their ability to well describe the nuclear structure observables in the stable region, we can now generate the microscopic optical potential directly from the effective phenomenological interactions.

According to Refs. [10, 18–20], the MOPs are given as

$$V_{\rm opt} = V_{\rm HF} + \Delta\Sigma(\omega), \tag{9}$$

where

$$\Delta\Sigma(\omega) = \Sigma(\omega) - \frac{1}{2}\Sigma^{(2)}(\omega). \tag{10}$$

In Eqs. (9) and (10), $V_{\rm HF}$ is the real, local, momentum-dependent, energy independent Skyrme HF mean-field potential, and ω is the nucleon incident energy. The polarization potential, $\Delta\Sigma(\omega)$, is non-local, complex, and energy dependent. $\Sigma(\omega)$ is the contribution from the particle-hole correlations generated from a fully self-consistent particle-vibration coupling (PVC) calculations [10, 18] applied on top of the collective states at small amplitudes generated by the Random Phase Approximation. The imaginary part of $\Sigma(\omega)$ is responsible for a loss of the incident flux due to the existence of nonelastic channels. $\Sigma^{(2)}(\omega)$ is the second-order potential generated from uncorrelated particle-hole contributions.

Using the partial wave expansion, the partial wave decomposition of the self-energy is

$$\Sigma_{lj}(r, r', \omega) = \hat{j} \sum_{\epsilon_\alpha, \epsilon_\beta} \frac{u_{lj}^{(\epsilon_\alpha)}(r)}{r} \Sigma_{\alpha\beta}^{(lj)}(\omega) \frac{u_{lj}^{(\epsilon_\beta)}(r')}{r'}, \tag{11}$$

where $\hat{j} = (2j+1)^{1/2}$. The self-energy is non-local, energy-dependent, complex and in separable form. These models have been used to reproduce the experimental data without ad hoc adjusted parameters on nucleon elastic scattering [10] by ^{208}Pb, neutron elastic scattering [13] by ^{16}O, proton inelastic scattering [14] by ^{24}O, nucleon elastic scattering by ^{40}Ca and ^{48}Ca [15–17], and nucleon elastic scattering [18, 19] by ^{16}O, ^{40}Ca, ^{48}Ca, and ^{208}Pb in the framework of the NSM (mostly with the Gogny and Skyrme interaction). However, the intricate disagreement with experimental data at backward angles is still exists.

Recently, we have used this model to analyze the effects of the spin-orbit and velocity dependent terms on the nuclear reactions observables. The obtained results are quite interesting. We have shown that the velocity dependent terms have strong effects on the surface while the spin-orbit term contributes in the interior region [20]. We assume in the near future to evaluate the sensitivity of the angular distributions and analyzing powers on each parameters of the Skyrme interactions. For example, in Figure 1, the sensitivity of the angular distributions of the neutron elastic scattering at low-energy on the choice of the interaction. The obtained results show this sensitivity is very small between the SLy5 and SkM* effective

interactions. More systematic calculations should be done in the near future. For the next step, the role of each the multipolarities to the imaginary part will be analyzed. These important information will be used to build up the new generation of optical potential.

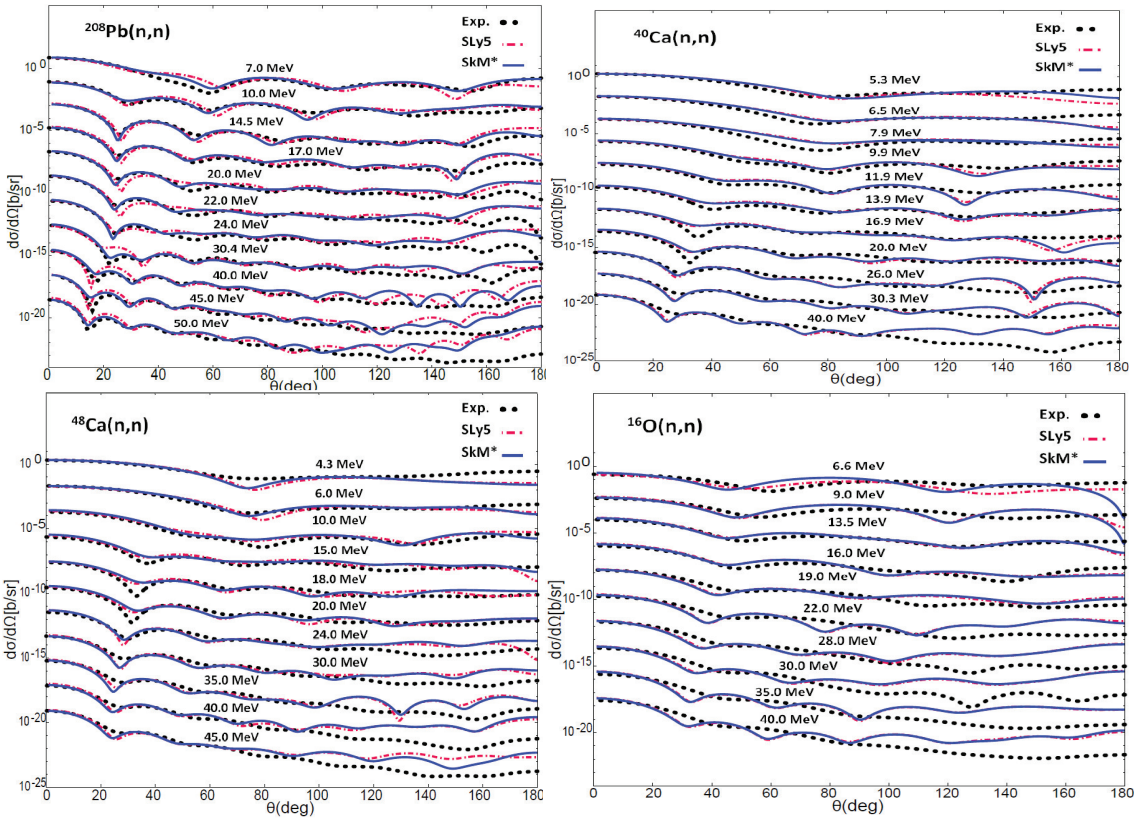

Fig. 1: Angular distributions of neutron elastic scattering by ^{16}O, ^{40}Ca, ^{48}Ca, and ^{208}Pb at different incident energies below 50 MeV. The solid (dashed) curve show the results of the MOP calculations using the SLy5 (SkM*) interaction. The results for SLy5 interaction are extracted from Ref. [19]. The experimental data are the tabulated cross sections taken from Ref. [21].

In conclusions, the microscopic optical potential is expected to be the vehicle to study the nuclear reactions in the unstable regions. However, the main challenging of this kind of potential is the precision is not high compared with the phenomenological one even in the stable region. As well known, this is due to the too complicated many body problem underlying. Therefore, the combination between the phenomenological and microscopic optical potential could be a promising

research direction.

ACKNOWLEDGMENTS

This work is funded by the Vietnam National Foundation for Science and Technology Development (NAFOSTED) under Grant No. 103.04-2018.303.

References

1. A. Idini, C. Barbieri, P. Navratil, Phys. Rev. Lett. **123**, 092501 (2019).
2. J. Rotureau, P. Danielewicz, G. Hagen, G. R. Jansen, F. M. Nunes, Phys. Rev. C **98**, 044625 (2018).
3. T. R. Whitehead, Y. Lim, J. W. Holt, Phys. Rev. C **100**, 014601 (2019).
4. J. W. Holt, N. Kaiser, G. A. Miller, Phys. Rev. C **93**, 064603 (2016).
5. J.-P. Jeukenne, A. Lejeune, and C. Mahaux, *Phys. Rev. C* **16** (1977), 80.
6. C. Barbieri, and B. K. Jennings, *Phys. Rev. C* **72** (2005), 014613.
7. H. F. Arellano, H. V. von Geramb, *Phys. Rev. C* **66** (2002), 024602.
8. M. Dupuis, S. Karataglidis, E. Bauge, J. P. Delaroche, and D. Gogny, *Phys. Rev. C* **73** (2006), 014605.
9. N. Vinh Mau, and A. Bouyssy, *Nucl. Phys. A* **257** (1976), 189.
10. V. Bernard, and N. Van Giai, *Nucl. Phys. A* **327**, (1979).
11. G. P. A. Nobre, F. S. Dietrich, J. E. Escher, I. J. Thompson, M. Dupuis, J. Terasaki, and J. Engel, *Phys. Rev. Lett.* **105** (2010), 202502.
12. G. P. A. Nobre, F. S. Dietrich, J. E. Escher, I. J. Thompson, M. Dupuis, J. Terasaki, and J. Engel, *Phys. Rev. C* **84** (2011), 064609.
13. K. Mizuyama, and K. Ogata, *Phys. Rev. C* **86** (2012), 041603(R).
14. K. Mizuyama, K.Ogata, Phys. Rev. C **89**, 034620 (2014).
15. G. Blanchon, M. Dupuis, H. F. Arellano, and N. Vinh Mau, *Phys. Rev. C* **91** (2015), 014612.
16. G. Blanchon, M. Dupuis, H. F. Arellano, *Eur. Phys. J. A* **51** (2015), 165.
17. G. Blanchon, M. Dupuis, R. N. Bernard, and H. F. Arellano, *Eur. Phys. J. A* **53** (2017), 88.
18. T. V. Nhan Hao, Bui Minh Loc, Nguyen Hoang Phuc, Phys. Rev. C **92**, 014605 (2015).
19. T. V. Nhan Hao, N. Nhu Le, M. H. Koh, N. Quang Hung, N. N. Duy, Vinh N. T. Pham, N. Hoang Tung, Int. J. Mod. Phys. E **27**, 1850052 (2018).
20. N. Hoang Tung, D. Quang Tam, V. N. T. Pham, C. Lam Truong, T. V. Nhan Hao, Phys. Rev. C **102**, (2020) 034608.
21. Experimental data taken from the National Nuclear Data Center, Brookhaven National Laboratory Online Data Service, http://www.nndc.bnl.gov/ensdf/.